XA9743298

POST-TEST INVESTIGATION RESULT ON THE VVER-1000 FUEL TESTED UNDER SEVERE ACCIDENT CONDITIONS

XA9743298

A. GORYACHEV, Yu. SHTUCKERT, E. ZWIR, L. STUPINA
State Scientific Centre, Research Institute of Atomic Reactors,
Dimitrovgrad, Russian Federation

Abstract

The model bundle of VVER-type were tested under SFD condition in the out-of-pile CORA installation.

The objective of the test was to provide an information on the VVER-type fuel bundles behaviour under severe fuel damage accident conditions. Also it was assumed to compare the VVER-type bundle damage mechanisms with these experiensed in the PWR-type bundle tests with aim to confirm a possibility to use the various code systems, worked out for PWR as applied to VVER.

In order to ensure the possibility of the comparison of the calculated core degradation parameters with the real state of the tested bundle, some parameters have been measured on the bundle cross-sections under examination. Quantitative parameters of the bundle degradation have been evaluated by digital image processing of the bundle cross-sections. The obtained results are shown together with corresponding results obtained by the other paticipants of this investigation.

1.Introduction.

In 1993 two model bundles of VVER type were tested under severe core accident conditions including the bundle element melting. The planning and execution of the experiments have been carried out by a cooperative effort of Forschungszentrum Karlsruhe (FZK), Karlsruhe (formerly Kernforschungzentrum, KfK), Nuclear Safety Institute of the Russian Research Center "Kurchatov-Institute" (RRC "KI"), Moscow, Research Institute "Luch" Scientific and Industrial Association (SIA "Luch"), Podolsk and Bochvar Research Institute of Inorganic Materials (RIIM), Moscow.

The model bundle tests were carried out in the out-of-pile installation CORA (KfK). During the tests the model bundles were subjected to temperature transients of a slow heatup rate in a steam environment and experienced a temperature escalations due to the exotermal zirconium-steam reaction. After the experiments the bundles were encapsulated with epoxy resin and cut to the cross-sectional samples. Polished sumples were distributed to the Russian laboratories RRC "KI", RIIM, Research Institute of Atomic Reactors (RIAR) and to the KfK for the posttest examinations. The model bundle CORA-W2 was subjected to the most detailed post-test examinations because of the experimental results of CORA-W2 test serve as a data base for comparison with analytical predictions of the high-temperature material behaviour by various code systems in the frame of International Standard Problem (ISP-36).

CORA-W2 cross-section post-test investigation was carried out in a joint effort by FZKA, RRS "KI", RIIM and RIAR. Detail description of the post-test examination results is presented in [1]. This paper describes some quantitative bundle damage parameters obtained from the cross-section microstructural posttest investigation.

2. Description of the CORA Test Facility and experiment procedure.

Detail description of CORA facility and experimental conditions are presented in [2]. In this chapter the main characteristics of the facility and experiment scenario are briefly described.

2.1. Description of the CORA Test Facility.

Out-of-pile CORA facility was designed to LWR bundle tests simulate the bundle heatup phase due to decay heat under the cooling by the superheated slow flow rate vapour of about atmospheric pressure.

The general view of CORA facility is presented in Fig.1, the facility flow diagram is shown in Fig.2. The central part of the facility is the fuel rod bundle. The CORA-W2 bundle was enclosed in a Zr-1%Nb shroud with ZrO_2 fibre insulation. Additional heat insulation of the bundle was provided by a high temperature radiation shield, that provided a flat radial temperature profile.

The steam was prodused in the steam generator. Jointly with an additional argon flow steam was superheated and guided to the lower end of the bundle. The steam not consumed within the bundle was condensed in two parallel condensors and the residual argon-hydrogen mixture was fed to the off-gas system after dilution with air to attain a low hydrogen concentration.

2.2. Bundle design.

The CORA-W2 model bundle consisted of 18 fuel rod simulators and one absorber rod simulator (Fig. 3). From the outside the fuel bundle was surrounded by the shroud of 1,0 mm thick Zr-1%Nb

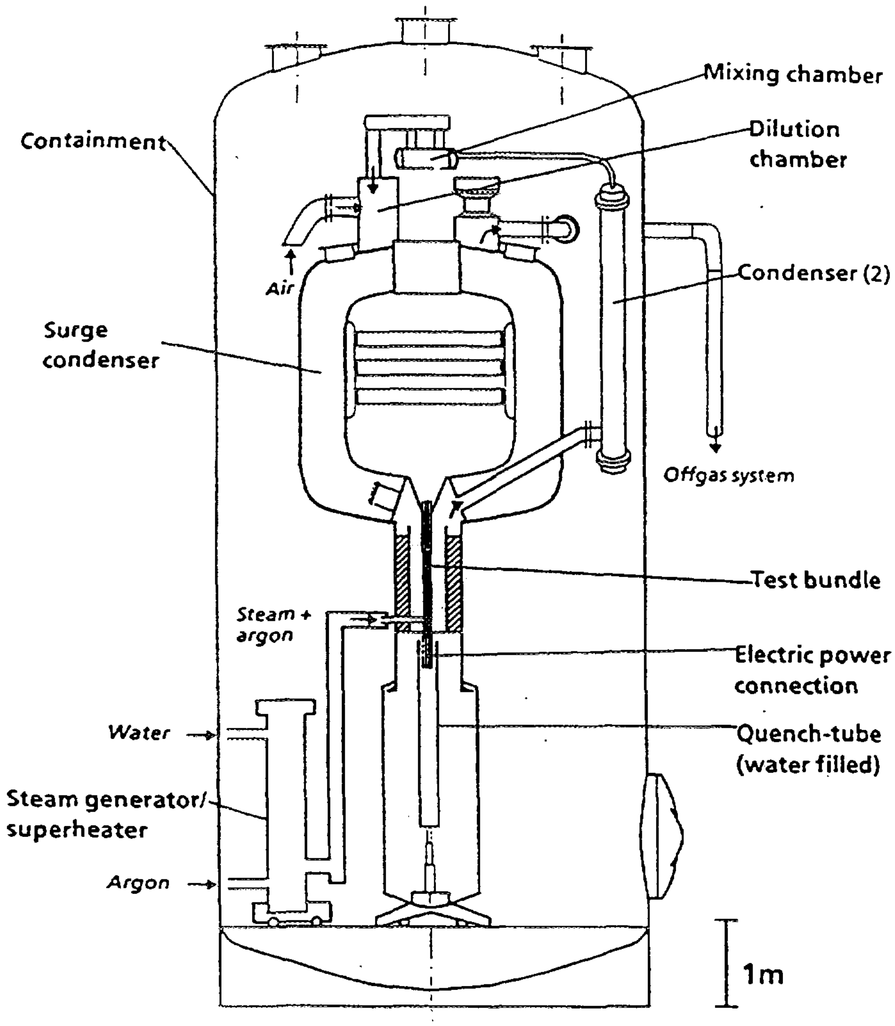

Fig. 1 SFD Test Facility CORA (Main components).

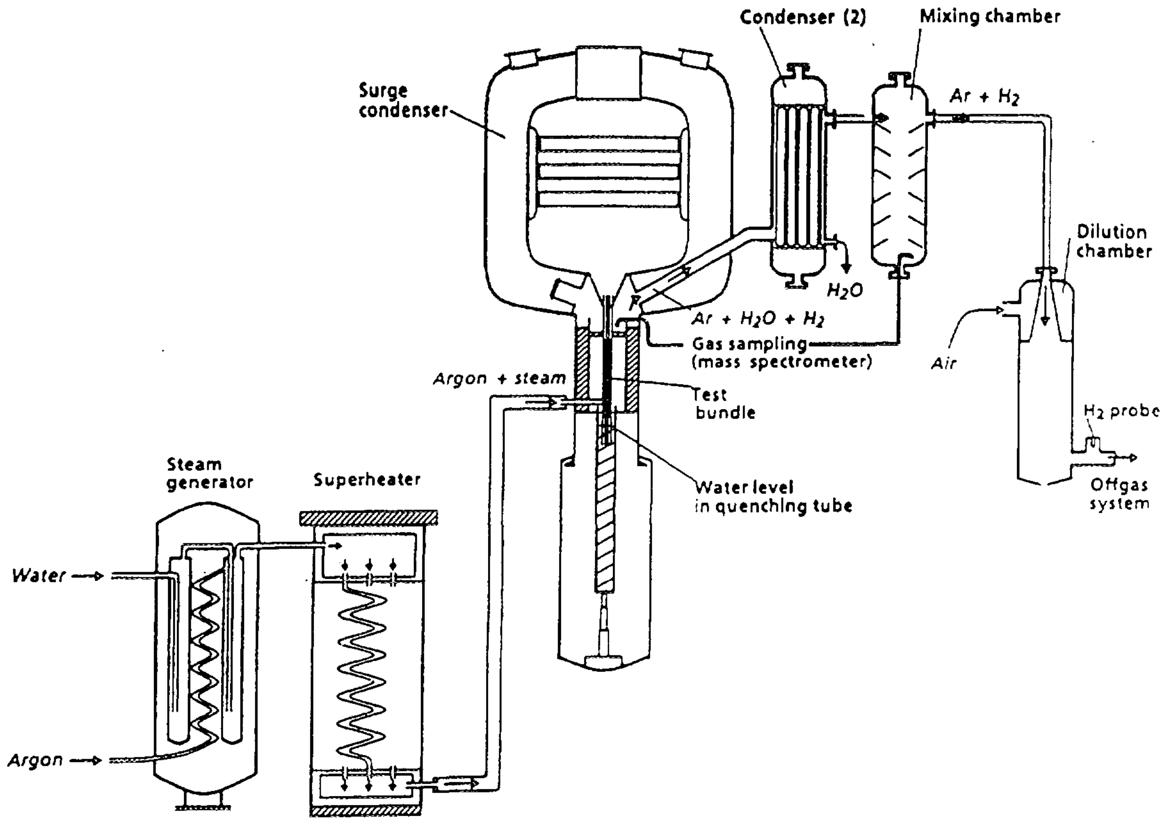

Fig. 2 SFD Test Facility (Simplified flow diagram).

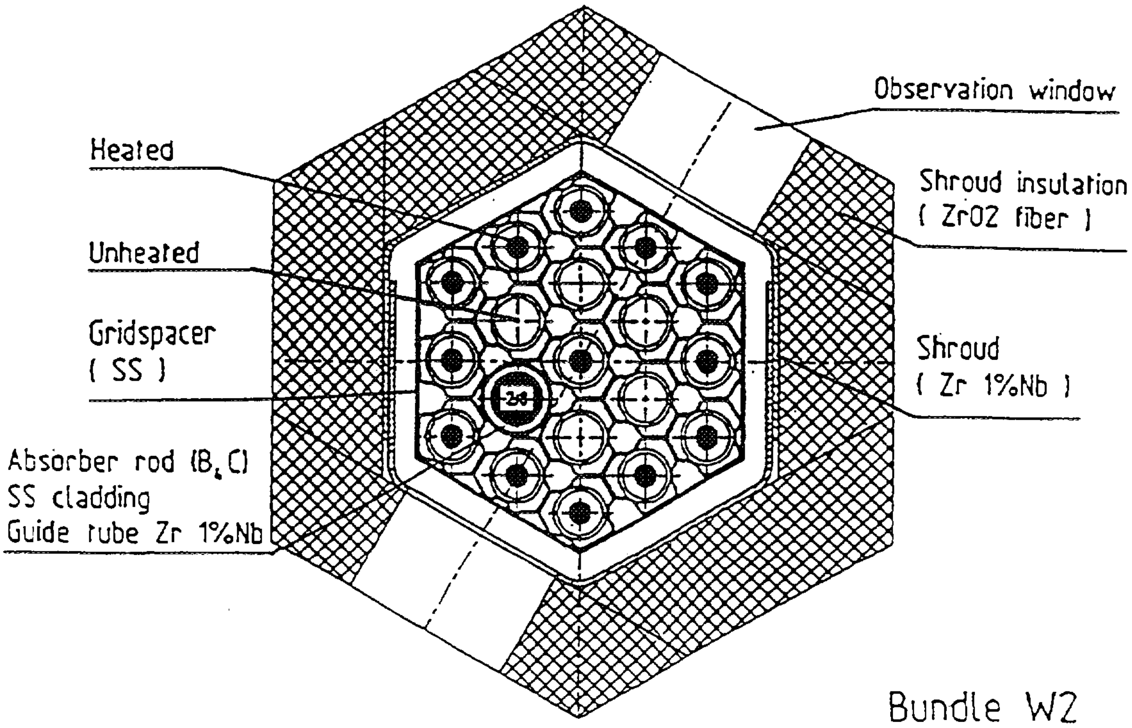

Fig. 3 Rod arrangement of bundle CORA-W2.

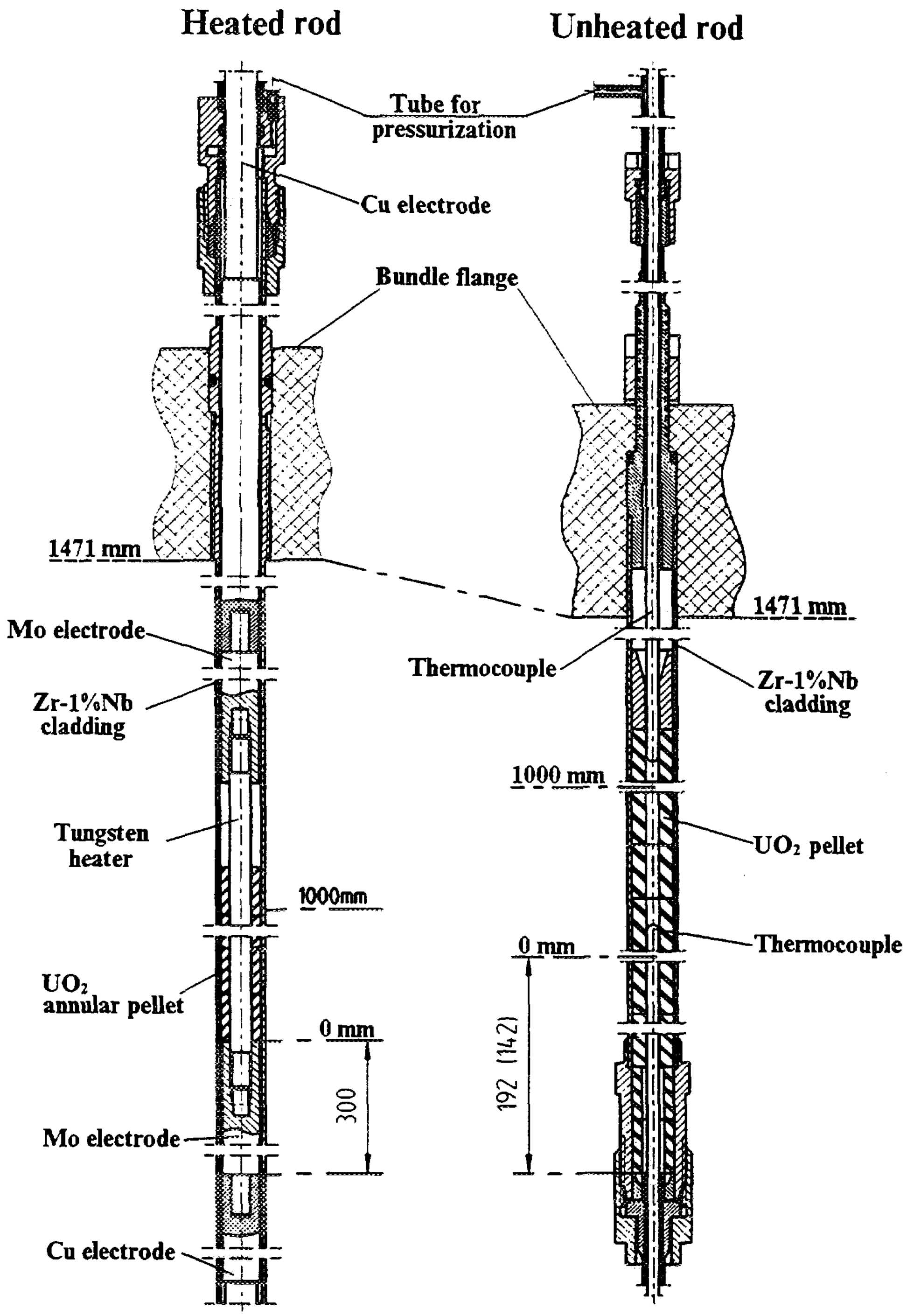

Fig.4 Rod types used in the CORA/WWER experiments.

alloy. The fuel element simulators were spased inside the shroud by means of three steel spacing grids manufactured according to the standard VVER-1000 technology and installed at marks - 5; 210; 610 mm. From the outer side the assembly shroud was equipped with the shroud insulation of fiber zirconium dioxide, that included two holes for the video monitoring of the experimental process.

The model CORA-W2 assembly used two types of fuel elements (Fig.4):

- heated rods - 13
- unheated rods - 5

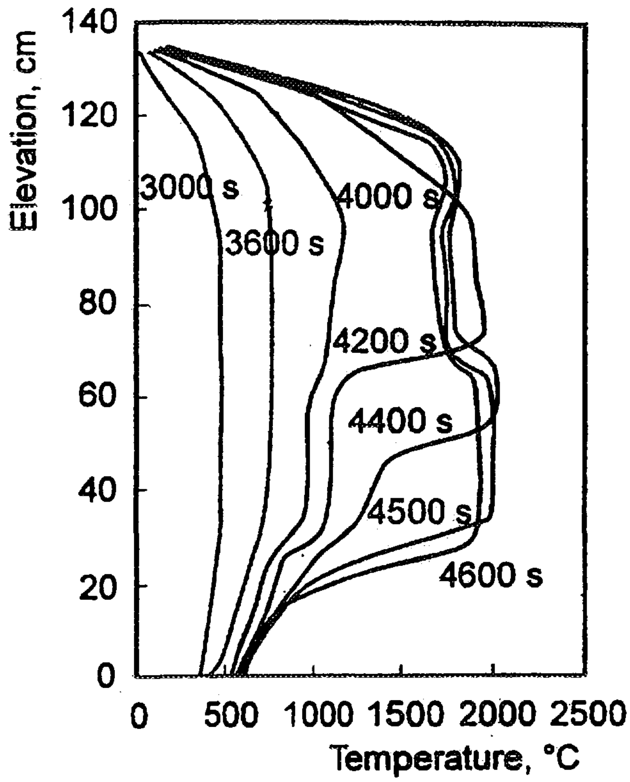

Fig.5 Axial temperature distribution along CORA/WWER-2 bundle.

The unheated rod simulators were of standard VVER-1000 design, radial dimensions and material composition. The column of fuel pellets in each of the heated rod simulators had the axial hole of 4.2 mm in diameter, where tungsten cylindrical heater of 4.0 mm in diameter was positioned.

The absorber rod consisted of the stainless steel guide tube and vibro compacted B_4C column in the SS cladding of standard VVER-1000 design.

2.3. Test Conduct and Initial Boundary Conditions.

The experiment scenario consisted of the following main phases:

1. 0-3000 s: pre heating of the assembly;
2. 3000-4500 s: heating phase;
3. 4500 s onwards: cooling phase.

During the first phase of the experiment, the pre-heated argon was supplied to the assembly at the flow rate of 8 $^{g}/s$ and low assembly electrical power of 0.5 kW. As a result the insulation temperature reached the level sufficient to prevent the vapour condensation. At 2760 s the argon flow rate was decreased to 6 $^{g}/s$. At time of 3300 s the steam started to be supplied to the assembly at the flow rate of 4 $^{g}/s$.

During the heating phase the bundle temperature was increased at the rate of about 1 $^{K}/s$ due to the electric power was increased from 2 kW to 14.5 kW. Experiment was terminated at 4500 s by the electrical heating switch off and termination of the steam supply.

The bundle axial temperature profiles is shown in the Fig.5.

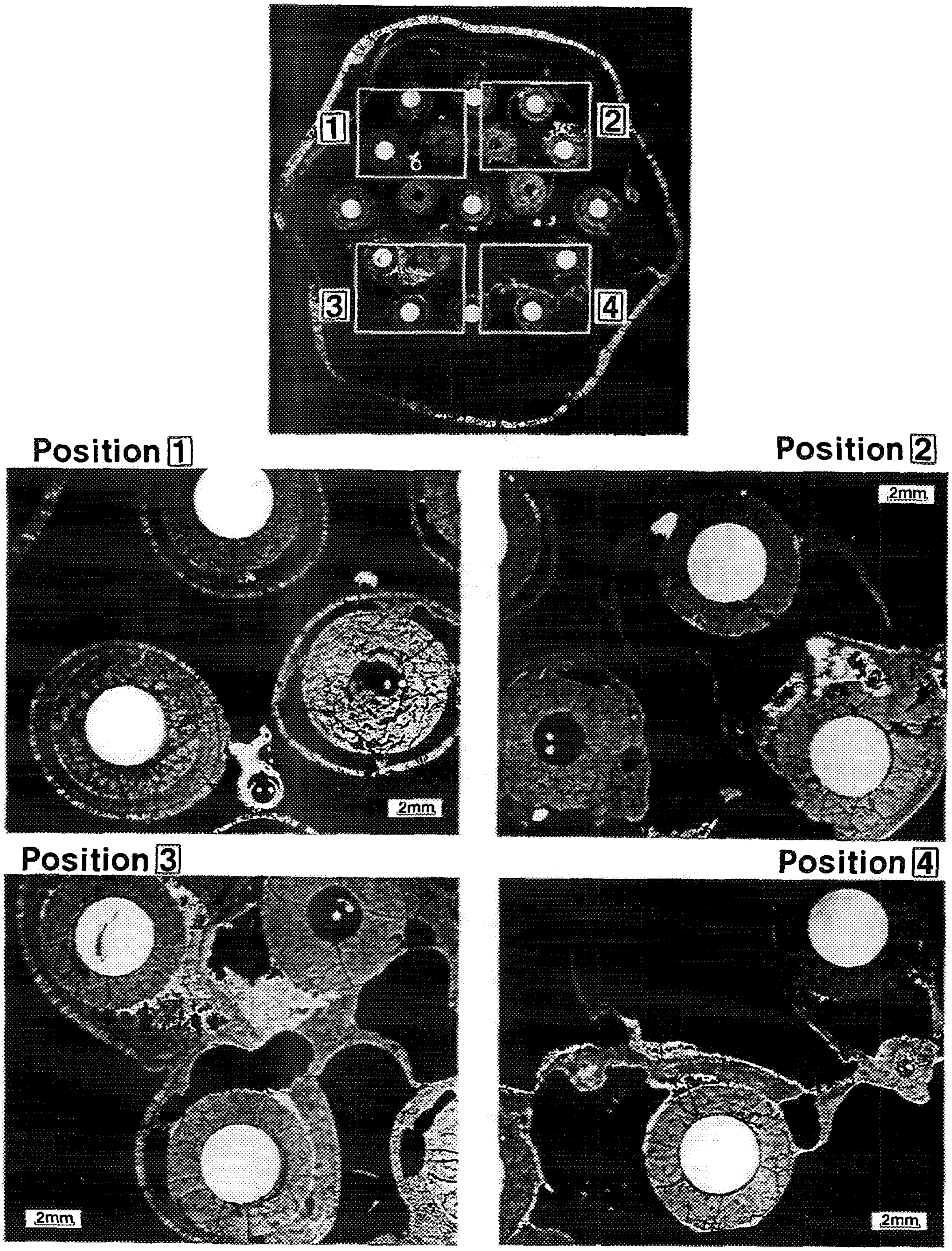

Fig.6. Cross-section W2-03 (bottom view).
Elevation 327mm.

3. Posttest appearance of the fuel rod simulators.

The example of the bundle cross section, that was cut out at the 327 mm elevation, where the bundle materials were almost completely oxidized, is shown in the Fig. 6.

According to the results of the bundle cross-sections posttest microstructural investigation the next conclusion on the high temperature simulator damage mechanism may be done.

During the heating phase of the experiment the ZrO_2 layers were formed on the simulator cladding surfaces. After the melting point temperature of the Zr-1%Nb cladding have been reached, the internal metallic layer of the cladding formed a melt, that begun to dissolve the fuel pellet and outer ZrO_2 layer. The formed melt can flow in the gap between the pellet and outer oxide layer, that led to the ZrO_2 layer deformation (Fig.6, Pos.1).

The final appearance of the simulator is a result of two competitive processes: melt oxidation due to oxygen uptake from the vapour and outer ZrO_2 layer dissolution. In the case of the outer oxide layer is not sufficiently thick, it is ruptured and liquid melt flow down on the simulator surface (Fig.6, Pos. 3). Following oxidation of the inner cladding surface lead to the flattening of the cladding, so called "flowering" (Fig.6, Pos.2). In the other case the liquid melt is completely oxidized in the gap between the fuel pellet and outer ZrO_2 layer (Fig.6, Pos.1).

A strong impact on the fuel rod simulator damage process have an interaction of the cladding and stainless steel, that lead to the eutectic formation with a melting point ($\sim 1200°C$) far below the melting point of Zr-1%Nb alloy. This interaction lead to the more intensive process of the outer ZrO_2 layer dissolution and cladding damage (Fig.6, Pos.4).

In general, the cladding failure mechanisms revealed in the CORA-W2 bundle test is very similar to those experienced in the PWR model bundle tests [3].

4. Quantitative measurements of the bundle damage parameters.

Quantitative estimation of the bundle damage parameters was made on the basis of the bundle structural element and melted material phase area measurements by means of the cross-section fragment image processing. In Fig.7 the example of the cross-section fragment image processing is shown. The phase types selected for the quantitative analysis is also shown in this figure.

As a result of the various phase cross-section area measurements the following parameters were estimated:

- core blockage formation;
- fuel pellets dissolution by the cladding melt;
- axial distribution of cladding oxidation;
- axial distribution of core melt.

4.1. Core blockage formation.

In order to evaluate a core blockage formation the total core material area was measured on each of the tested cross-sections. Materials, were identified as belonging to the bundle shroud, were not taken into account. The bundle cross-sectional area axial distribution is shown in the Fig.8.

These data reflect only an area occupied by the bundle material excluding material porosity. Therefore, the cross-sectional area available for the vapour flow may be overestimated, because of some of the pores, that may be seen on the cross-sections, may appear to be the closed pores inside a bundle material and their cross-sectional area are not available for a vapour flow. In view of this assumption the additional measurements were made. In this case the area of pores, which look like

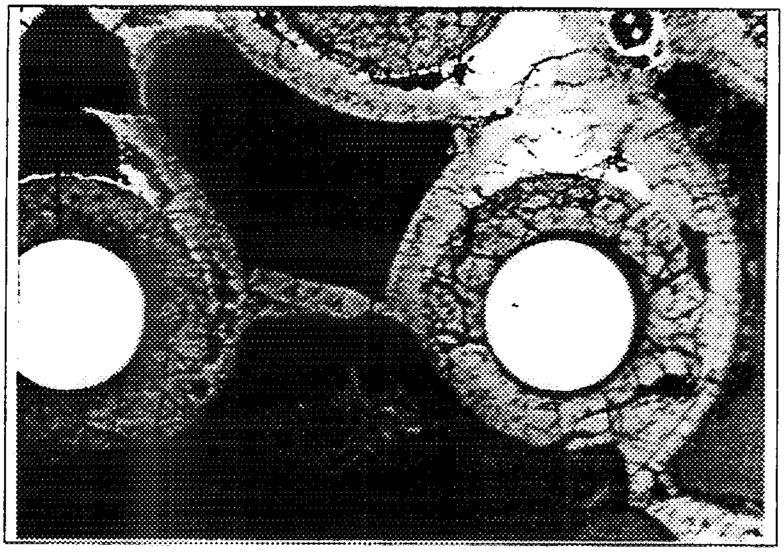

Original view

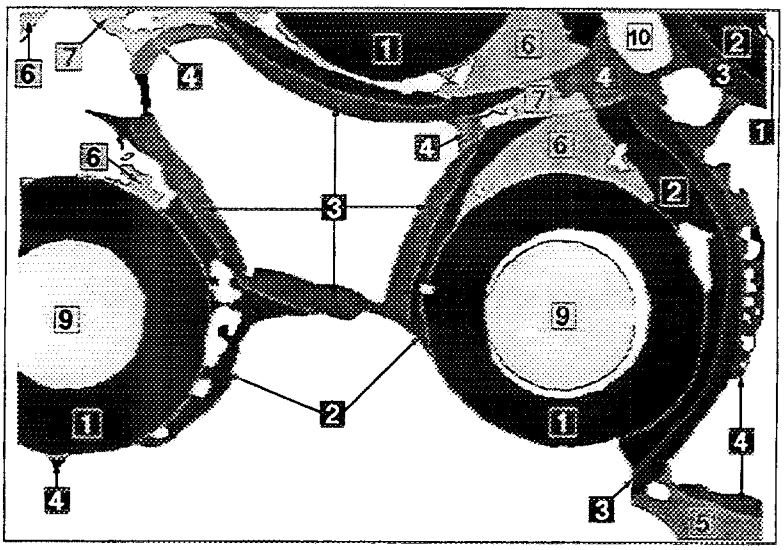

View reformed for analysis

1 Pellet remnants	6 Metallic melt
2 Oxidized melt	7 Metallic melt
3 ZrO_2 layer	8 Metallic phase of the shroud
4 Oxidized melt	9 Tungsten heater
5 Oxidized shroud	10 Thermocouple

Fig.7 Image processing of the cross-section fragment.

closed in the cross-section, i.e. have no visible leakage to the area among the fuel rod simulators, was added to the core material area. The resulting data is also shown in the Fig.8. Obviously, two group of the obtained data represent the extreme estimations. The real value of the core blockage must be in the range limited by these estimations.

As can be seen from the Fig.8, the axial redistribution of the core melt led to creation of two local core blockages at the marks correspond to the positions of the spacer grids. The lower blockage is created by the stainless steel melt originated from the absorber rod cladding and guide tube and contains a small amount of uranium and zirconium. The upper blockage is created by the melt, originated from the fuel rod simulators material, and is significantly polluted by the stainless steel components.

The remarkable fact is, that despite of the upper spacer grid was completely melted early in the bundle temperature ramp, it affected on the following core melt redistribution.

In general, CORA-W2 bundle material redistribution is of the same character that was observed in the absorber material bearing PWR model bundles tests.

4.2. ZrO_2 axial distribution and cladding oxidation profile.

In order to evaluate the cladding oxidation and final ZrO_2 distribution the zirconia layers area was measured on the bundle cross-sections. The results is shown in the Fig. 9. It should be taken into account that this data reflect only area of the ZrO_2 layers formed on the outer cladding surfaces during solid state oxidation of the claddings. In the most cases this outer oxide layers retained only partially due to mechanical failure and dissolution by the melt. In order to obtain a more realistic picture of the cladding oxidation profile formed during the solid state oxidation phase, the measurements of the average oxide film thickness was made. The thickness of the zirconia layers or their remnants were calculated as a ratio of the each measured object area to the half of its perimeter. As a result the average thickness of each measured layer were obtained. The result is not influensed by the missing of the some parts of the oxide layer from the cladding surface. The results of this measurements is shown in the Fig. 10. In the upper cross-sections of the bundle cladding oxidation have a smooth profile. The extreme value at the mark of 270 mm may be explained by the fact, that in this cross-section the cladding melting point temperature was reached late, than in the upper cross-sections and therefore, the solid state oxidation phase were longer.

4.3. Fuel pellets dissolution.

In order to evaluate the final uranium redistribution along the bundle the fuel pellet remnants area was measured in the each cross-section. The results of the fuel pellet remnants area measurements is shown in the Fig. 11. It should be noted, that no any fuel pellet damage mechanisms other than pellet dissolution by the melt were observed in the course of the microstructural investigations. The comparison of the heated and unheated simulator fuel pellets dissolution is shown in the Fig. 12. The averaged over the cross-section fuel pellet dissolution is not exceed of 17 %, but the fuel pellets of the individual simulators were experiensed a dissolution to a great extent, that, obviously, may be explained by the non uniform radial distribution of the melt in the bundle.

4.4. Axial distribution at the core melt.

The cross-sectional area of the melted material, that have not been definitely attributed to any of initial materials of the bundle and consisted of the complex mixture of the initial bundle materials, was measured in order to evaluate the core blockage formation and final core material distribution. The results of the measurements are shown in the Fig. 13. In order to

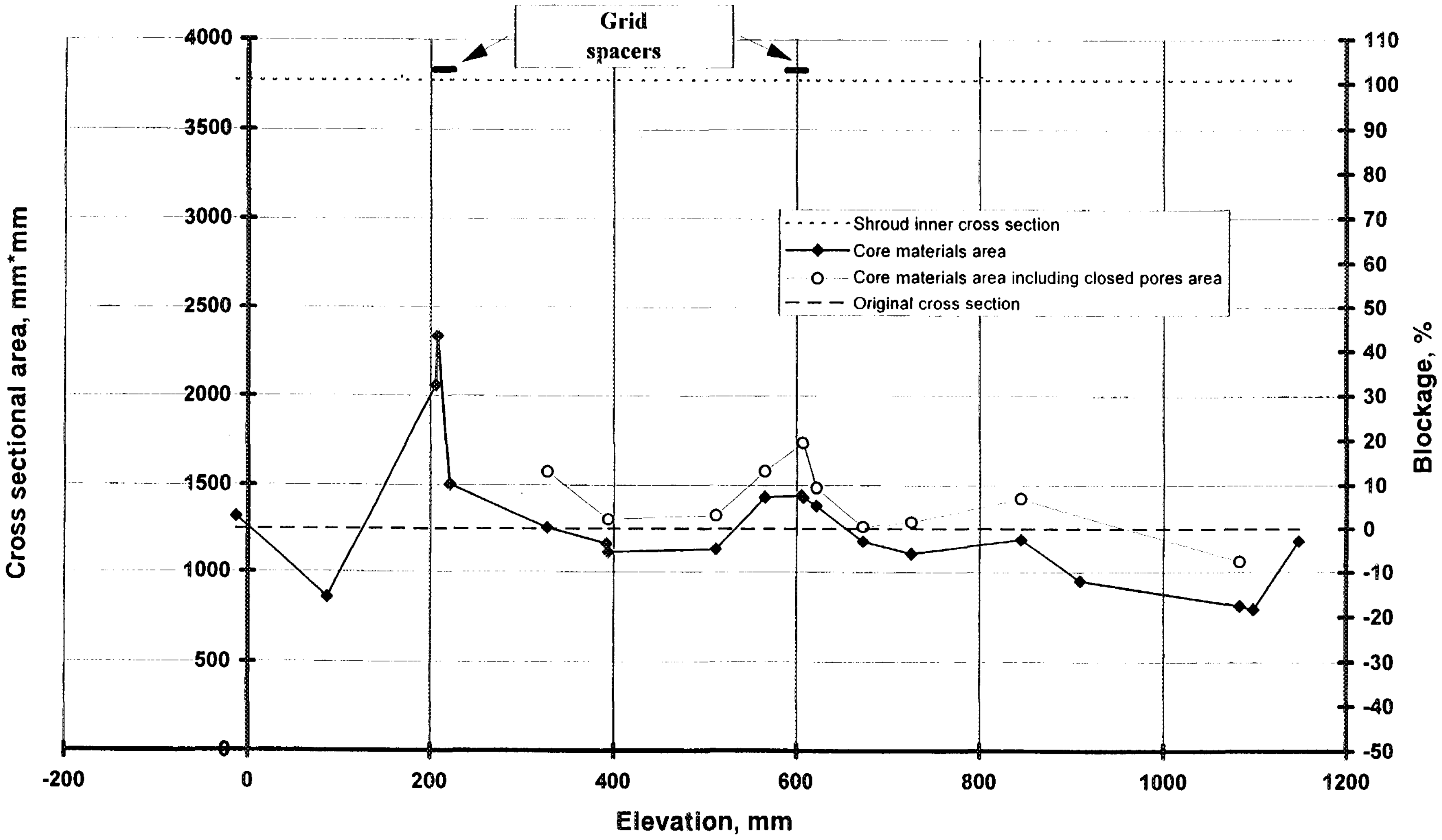

Fig.8 Profile of the cross-sectional areas after test CORA-W2.

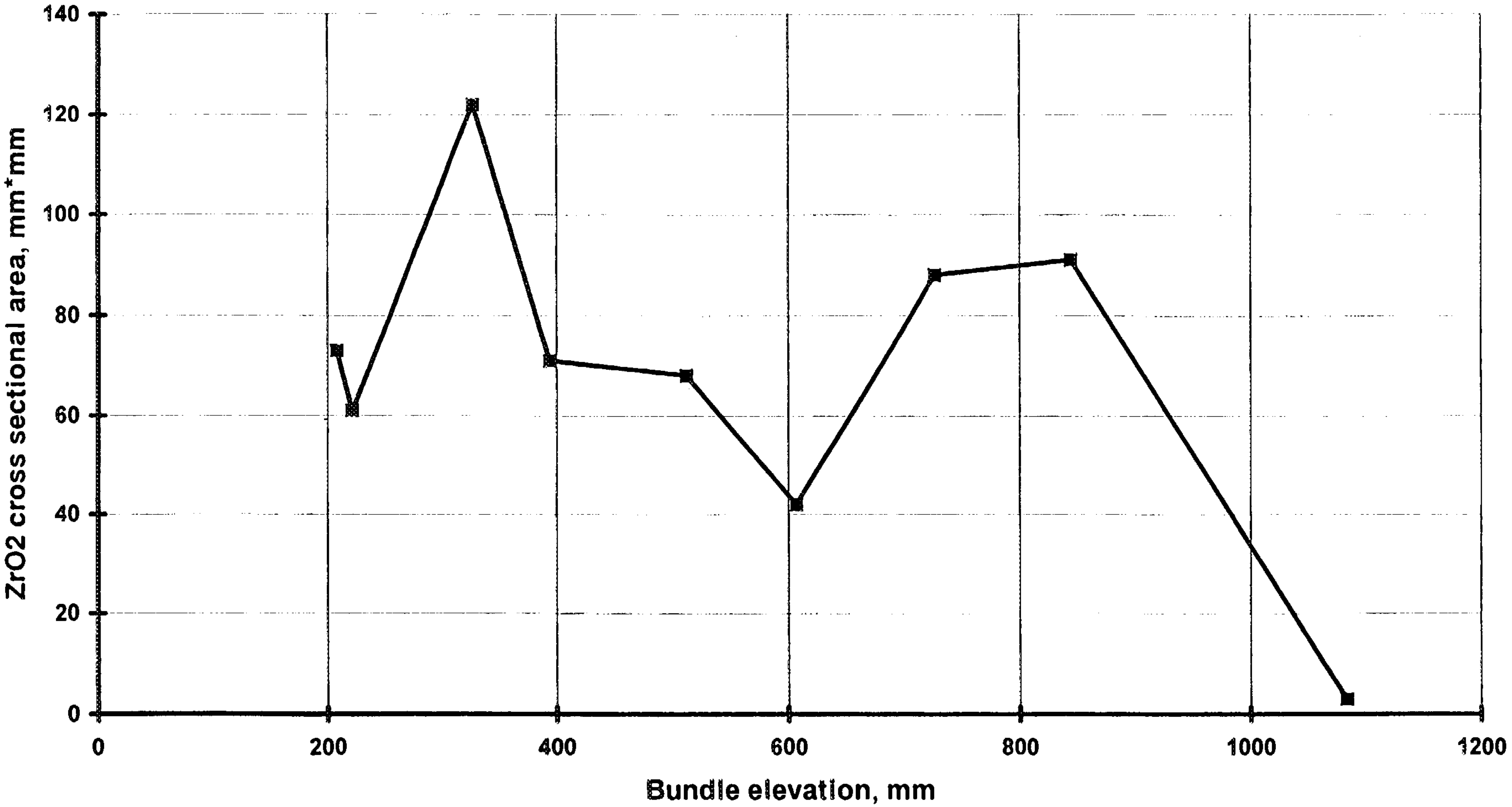

Fig.9 Axial profile of the remained cladding ZrO2 scales cross sectional area.

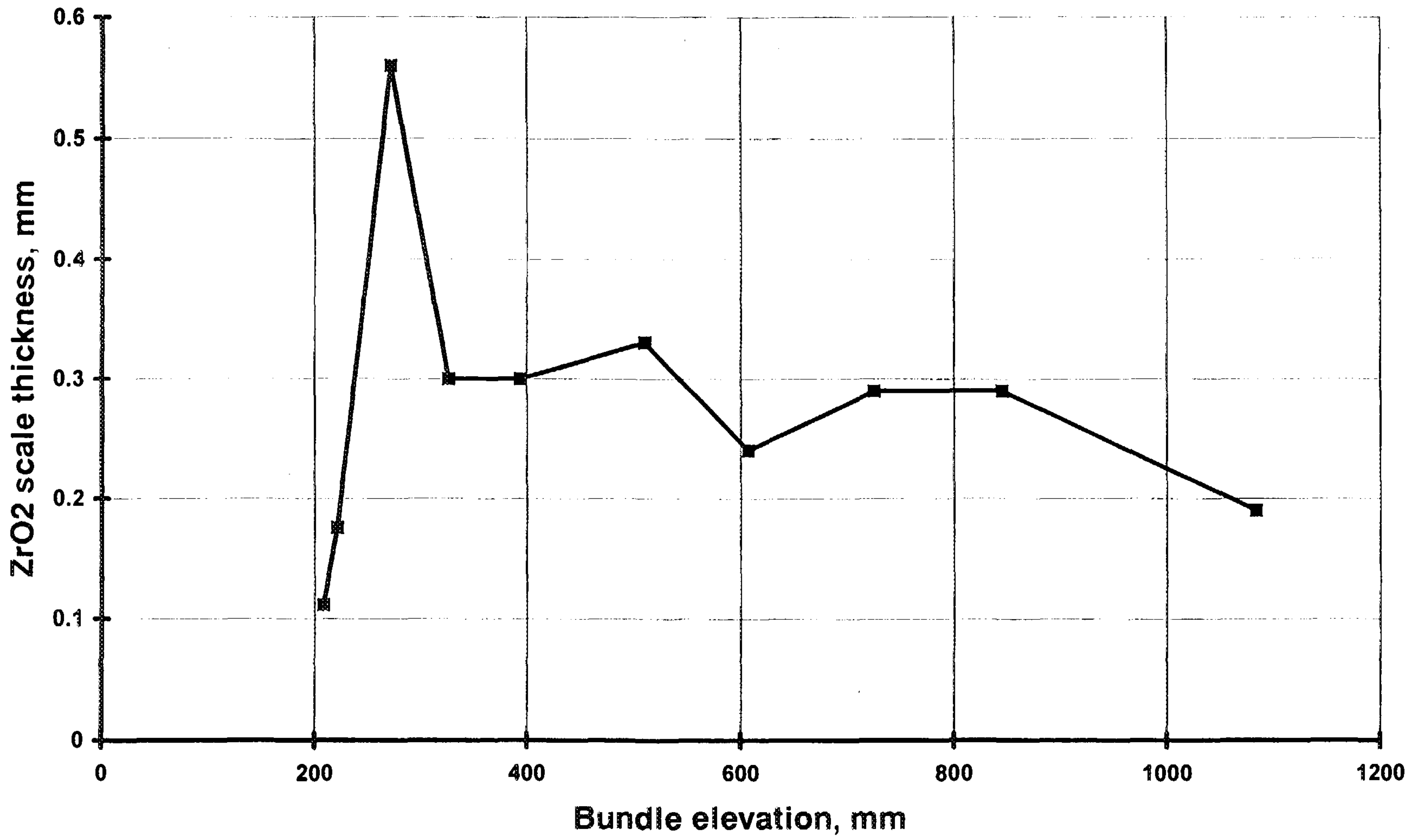

Fig.10 Profile of cladding oxidation along the bundle CORA-W2.

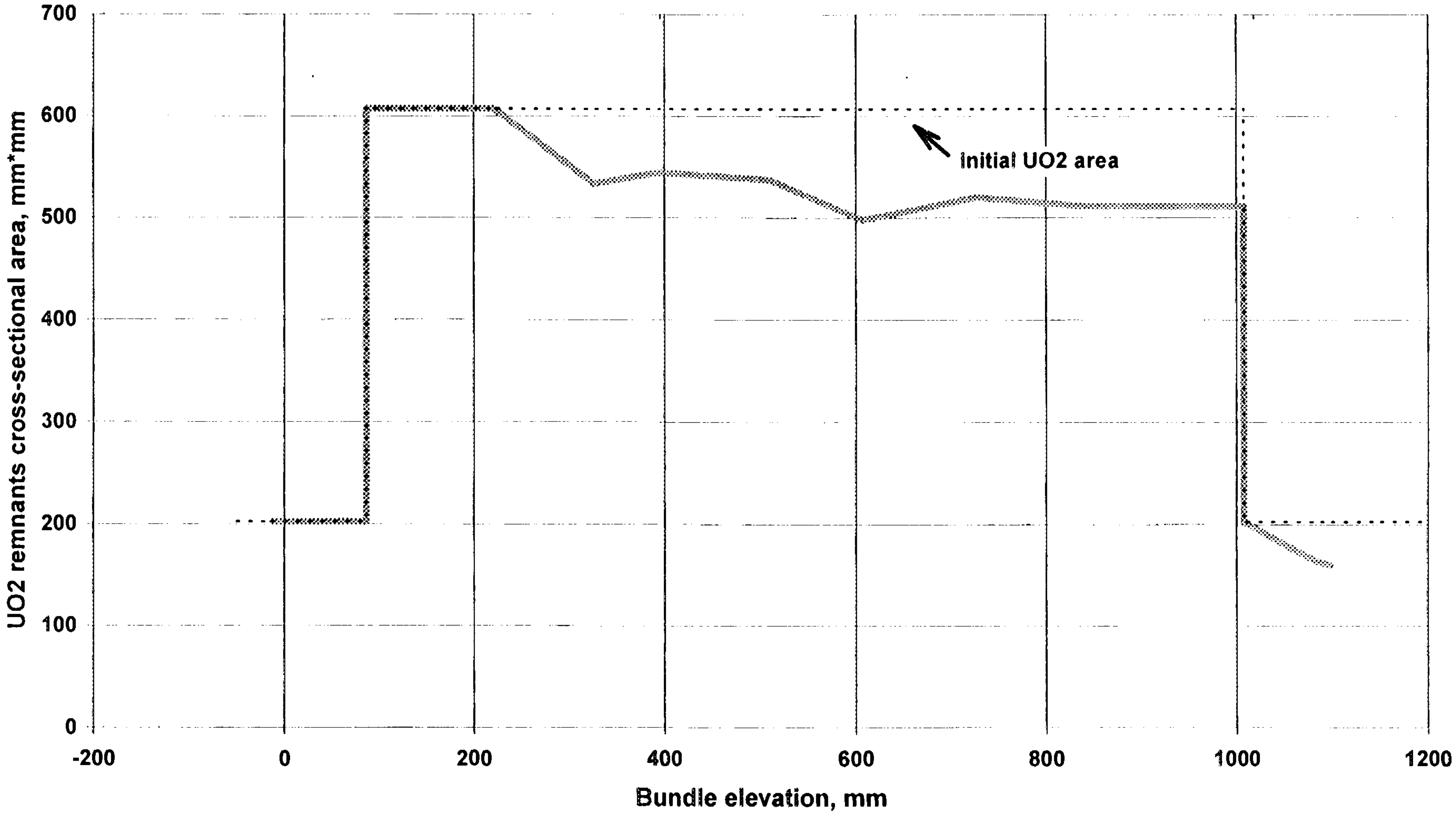

Fig.11 Axial profile of the UO2 pellets cross sectional area after the test CORA-W2.

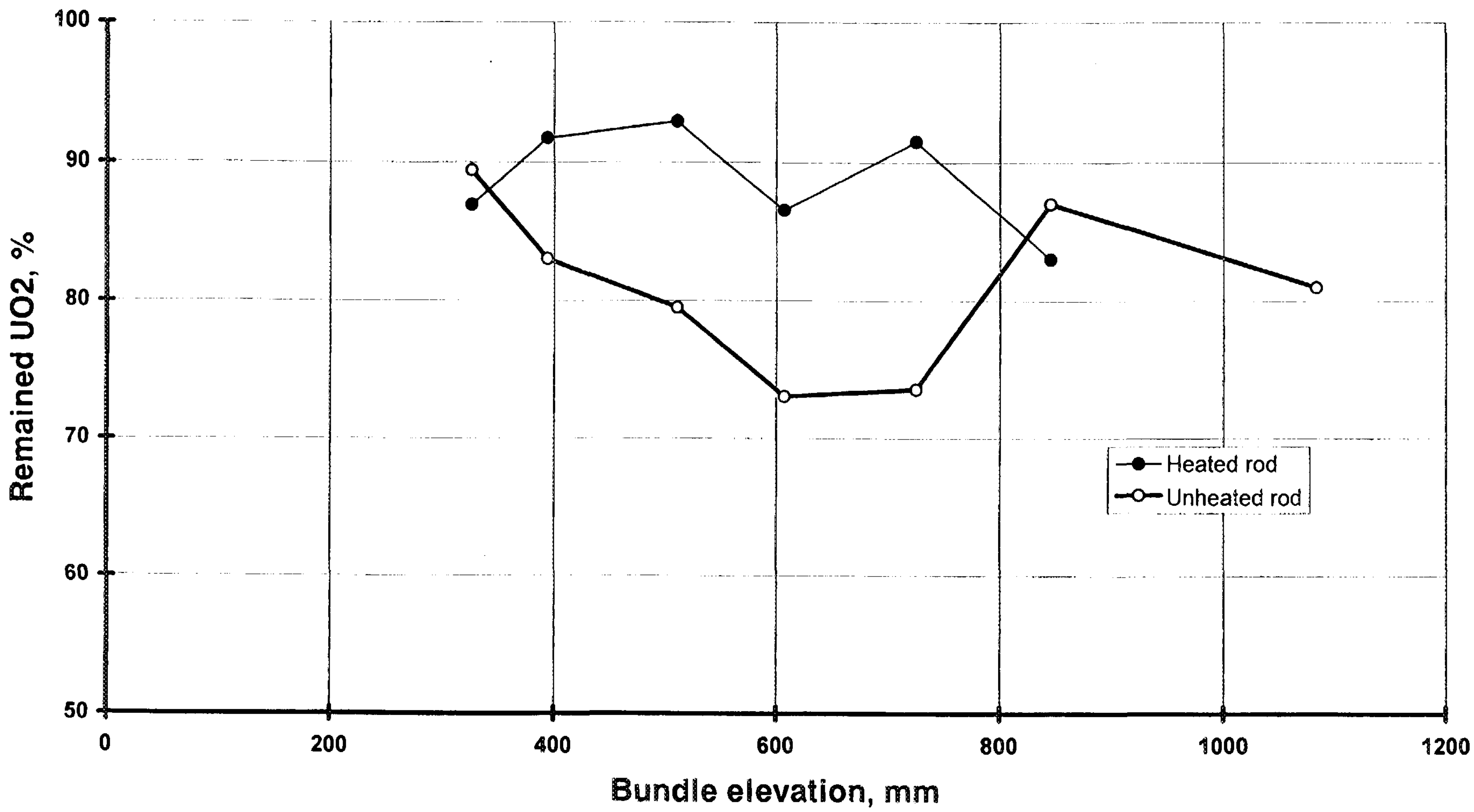

Fig.12 Damage profile of UO2 pellets.

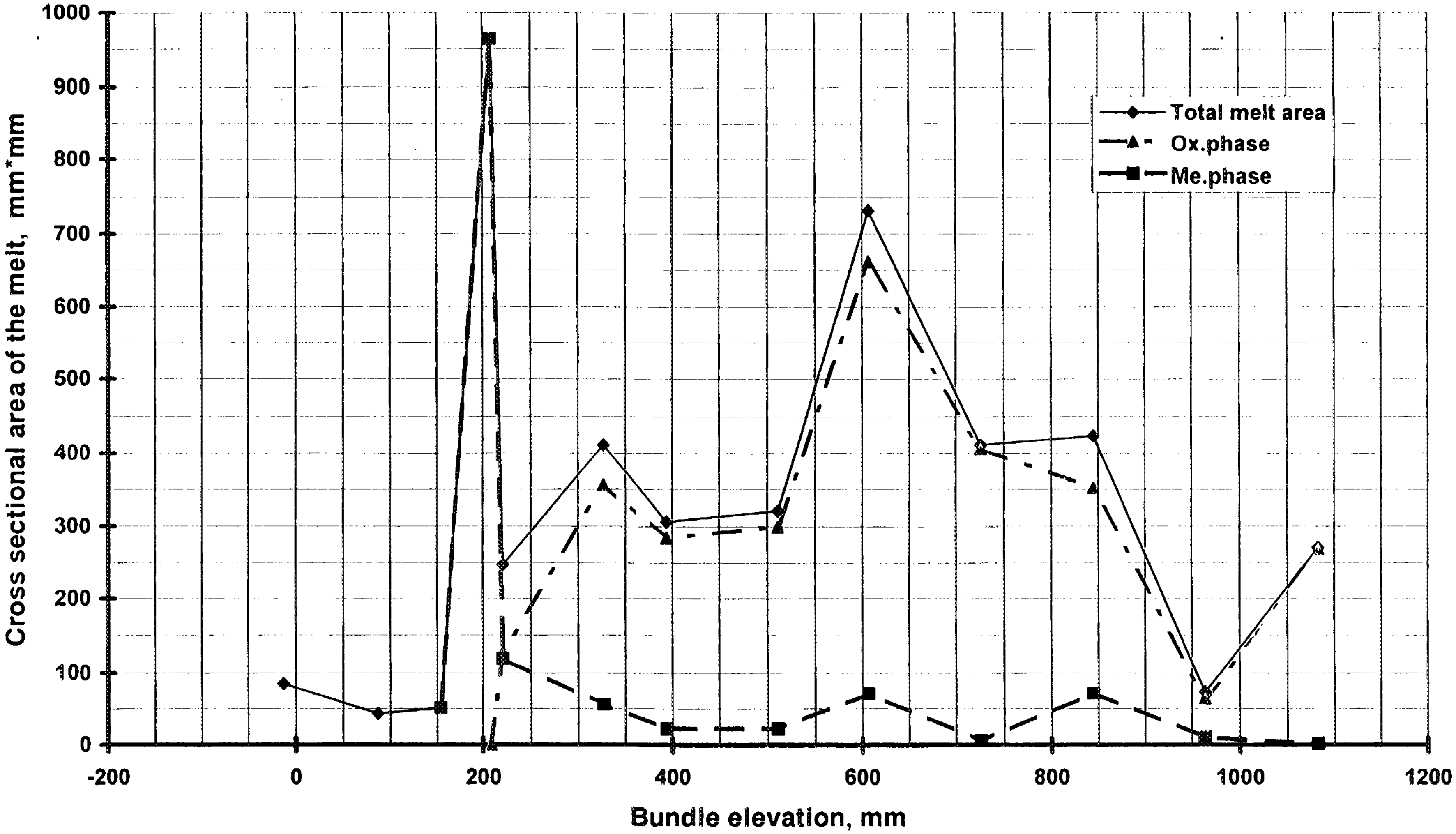

Fig.13 Axial profile of the core materials melt cross-sectional area.

estimate a relocated melt oxidation the cross-sectional area or the oxidized and metallic parts of the melt were measured separately. In the case of the
phase under investigation consisted of the metallic and ceramic grains mixture, the image analysis of the microstructures was used for separation of the metallic and oxidized parts of this phase.
As one can see from the Fig. 13, the main part of the relocated melt were oxidized and most likely, that core melt flowing finished before the end of the test. The metallic part of the melt consists mainly at the stainless steel melt, originated from the absorber rod cladding and guide tube, that formed a lower blockage, and separated stainless steel droplets remained in the oxidized matrix at the oxidized core melt in the upper part of the bundle.

Conclusions.

The data of the posttest microstructural investigations and quantitative parameter measurements present a consistent picture of the VVER-type bundle behavior under SFD conditions.

The experiment realized led to a better understanding of the severe fuel damage processes in the VVER core.

In general, the VVER fuel bundles behaviour in the early stage of the loss-of-coolant accident is similar to the behaviour of the PWR bundles.

The results obtained from the posttest bundle examination consist a data base for the comparison with the analytical predictions of the bundle behaviour by the codes.

REFERENCES

1. Posttest Examination of the VVER-1000 Fuel Rod Bundle CORA-W2,

FZKA 5570 (1995)

2. S. Hagen, P. Hofmann, V. Noack, G. Schanz, G. Schumacher, L. Sepold "Behavior of a VVER-1000 Fuel Element with Boron Carbide/Steel Absorber Tested under Severe Fuel Damage Conditions in the CORA Facility",

   KfK 5363 (1994).

3. K. Minato, W. Hering, S. Hagen "Zircaloy Oxidation and Cladding Deformation in PWR-Specific CORA Experiments", KfK 4827 (1991).